Physicochemical Characterization of 2-Hydroxybenzophenone with β-Cyclodextrin in Solution and Solid State

6 AUTHORS, INCLUDING:

Matias I. Sancho
Universidad Nacional de San Luis
17 PUBLICATIONS **88** CITATIONS

SEE PROFILE

Marcos G. Russo
5 PUBLICATIONS **2** CITATIONS

SEE PROFILE

Mario Sergio Moreno
Centro Atómico Bariloche
82 PUBLICATIONS **1,084** CITATIONS

SEE PROFILE

Griselda E Narda
Universidad Nacional de San Luis
47 PUBLICATIONS **348** CITATIONS

SEE PROFILE

Article

Physicochemical Characterization of 2-Hydroxybenzophenone with β-Cyclodextrin in Solution and Solid State

Matias I. Sancho,*,[†] Marcos G. Russo,[‡] M. Sergio Moreno,[§] Estela Gasull,[†] Sonia E. Blanco,[†] and Griselda E. Narda[‡]

[†]IMIBIO−CONICET. Área de Química Física, Facultad de Química, Bioquímica y Farmacia, and [‡]INTEQUI-CONICET. Química Inorgánica, Facultad de Química, Bioquímica y Farmacia, Universidad Nacional de San Luis, Chacabuco 917, San Luis 5700, Argentina

[§]Instituto Balseiro, Centro Atómico Bariloche, San Carlos de Bariloche 8400, Argentina

ⓢ *Supporting Information*

ABSTRACT: The characterization of the inclusion complex between 2-hydroxybenzophenone (2OHBP) and β-cyclodextrin (βCD) in the solid state was performed using Fourier transform infrared spectroscopy (FTIR), powder X-ray diffractometry (PXRD), differential scanning calorimetry (DSC), thermogravimetric analysis (TGA), and transmission electron microscopy (TEM). The apparent formation constant of the complex was determined by phase solubility diagrams and liquid chromatography (HPLC) at different temperatures. The formation of the inclusion complex induced slight shifts in the FTIR spectrum while by PXRD a new crystalline phase was observed. TEM studies revealed that the complex forms aggregates of nanometric size. The inclusion complex showed a higher solubility in the tested dissolution media than free 2OHBP. Moreover, the freeze-dried solid complex exhibits a higher thermal stability than the solid free drug. The thermodynamic analysis allowed us to conclude that the encapsulation process is endothermic in water and exothermic in methanol−water.
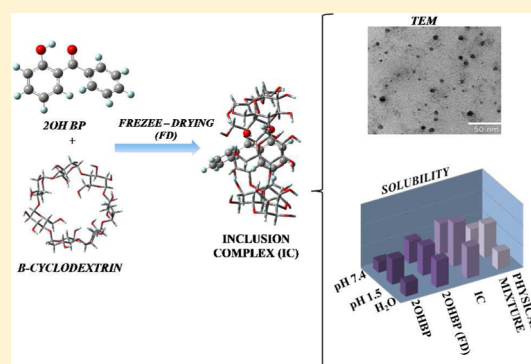
1. INTRODUCTION

Benzophenones (BPs) are diphenyl ketones, usually obtained from diverse natural products[1−3] or by chemical synthesis.[4] Among the existing BPs, hydroxybenzophenones represent a significant class of pharmaceutical compounds. They exhibit important biological properties, such as cytotoxic effects against different human cancer cells.[5,6] They also present inhibitory effects on xanthine oxidase, the enzyme responsible for the overproduction of uric acid and the subsequent hyperuricemia.[7] In particular, 2-hydroxybenzophenone (2OHBP, Scheme 1) and some of its derivatives exhibit strong anti-inflammatory effects[8,9] with low ulcer production activity. Additionally, significant antioxidant activity was reported for 2OHBP and their derivatives.[10] These compounds also present a wide variety of chemical properties. Because of their ability to absorb and dissipate UV radiation, BPs derivatives are used as

sunscreens lotions[11] or in the preparation of UV-protecting coats in food packages and other plastics.[12]

Despite the physicochemical relevance of these compounds, their use is rather limited due to their poor aqueous solubility and low thermal stability. Other undesirable effect is the estrogenic activity on some BPs, although 2OHBP is among the less active ones.[13] One of the most frequently employed methods to increase the aqueous solubility of a drug is the formation of inclusion complexes with cyclodextrins (CDs).[14−16] CDs are nontoxic macrocyclic sugars with a truncated cone shape, and they are formed by six, seven, or eight units of α-(1 → 4)-D-glucose per molecule (α, β, and γ CD, respectively). CDs are water-soluble, and hydrophobic drugs with appropriate size and shape can enter into the cavity, forming noncovalent supramolecular complexes.[17] The formation of these complexes not only enhances the aqueous solubility but in some cases also improves the general stability of the drug.[14] Additionally, it was also reported that βCD is able to suppress the strong estrogenic activity of some compounds.[18] For this reason, CDs have been extensively applied to pharmaceutical drugs formulation as excipients. Moreover, CDs and their inclusion complexes are able to self-assembly in

Scheme 1. Molecular Structure of 2-Hydroxybenzophenone

A
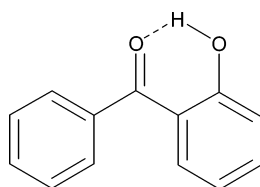
aqueous solution linked by intermolecular CD−CD H-bonds and form aggregates of higher size. These aggregates may have an important effect on the chemical and biological properties of the inclusion complexes, so the study of such aggregates is of great interest.[15,19]

In the present work, an experimental study of the inclusion process between 2OHBP and βCD in solution and solid state was conducted. The aim of this study was to identify possible interactions between these compounds, which, to best of our knowledge, they have not been reported yet. In addition, the goal of this study is also to improve physicochemical properties of the drug by complex formation with βCD. The solid state complex was prepared by the freeze-drying (FD) method. Appropriate combination of instrumental techniques were employed for the complex characterization, including Fourier transform infrared spectroscopy (FT-IR), differential scanning calorimetry (DSC), thermogravimetric analysis (TGA), X-ray diffractometry (XRD), and transmission electron microscopy (TEM). Equilibrium solubility of the pure drug and the inclusion complex was measured by the saturation *shake flask* method. Determination of the stoichiometry and apparent formation constants in aqueous solutions was carried out using phase-solubility diagrams obtained by UV−vis spectroscopy. The apparent formation constant was also determined in methanol−water solutions by means of a liquid chromatography (HPLC) method. Thermodynamic parameters were obtained from the relationship between the temperature and the formation constants. Finally, a molecular modeling analysis of the inclusion process between 2OHBP and βCD was performed to obtain information about the molecular geometry of the complex.

2. MATERIALS AND METHODS

2.1. Reagents. βCD was purchased from MP Biomedicals, and 2OHBP was purchased from Sigma-Aldrich Chemical Co.; they were used without further purification. HPLC grade methanol (MeOH) was acquired from Merck, and double distilled water was purified using a Thermo Scientific Easypure II system, with conductivity lower than 1.8 μS cm^{-1}. All the reagents employed in the preparation of the buffer solutions were of analytical grade.

2.2. Preparation of the Solid State 2OHBP:βCD Binary Samples. *2.2.1. Freeze-Drying (FD).* The sample was prepared by mixing equimolar amounts of the reagents (8 mM) in 100 mL of a mixed ethanol:water solution (1:1, v/v) with magnetic stirring at room temperature for 48 h protected from light to prevent degradation. The solution was then filtered with a 0.45 μm Millipore membrane, placed on stainless steel trays, frozen at −40 °C, and freeze-dried using a Rificor lyophilizer (model L-A-B4) for 48 h at 1 bar. The dried sample was placed in a close flask and stored in a sealed container with silica gel (relative humidity lower than 5%). In order to verify the influence of the FD on the aqueous solubility and structural features of 2OHBP, a solution of the pure drug was also submitted to this process. The storage time was less than 4 weeks for all the samples.

2.2.2. Physical Mixture (PM). The mixture was prepared by adding equimolar amounts of the reagents (2OHBP and βCD) into an agate mortar and gently grinding the mixture for 10 min at room temperature and humidity. The PM was stored as obtained (unsieved) under the same conditions that the FD samples. The reproducibility of the obtained phase was confirmed by powder X-ray diffraction. The PM sample was prepared as a reference for comparison purposes.

2.3. FT-IR Spectroscopy. Fourier transform infrared spectra were recorded on a Nicolet PROTÉGÉ 460 spectrometer (Nicolet Instrument Corporation, Madison, WI) provided with a CsI beamsplitter in the 4000−400 cm^{-1} range with 64 scans and spectral resolution of 2 cm^{-1} using the KBr pellet technique. Variable temperature Fourier transform infrared (VT-FTR) spectra were recorded using an accessory developed by Seasing SRL (La Plata, Argentina) which consists of a variable-temperature IR cell provided with KBr windows operating under high vacuum. The temperature controller allows the cell to collect spectra between room temperature and 250 °C.

2.4. Powder X-ray Diffraction. Powder X-ray diffraction diagrams (XRPD) were obtained in a Rigaku D-MAX IIIC (Rigaku Co, Tokio, Japan) diffractometer using Cu Kα radiation (Ni-filter) and NaCl and quartz as external calibration standards. The diffractograms were recorded in the 2θ angle range of 3°−50°, and the process parameters were set at 0.02 2θ scan step size and 2 s scan step time.

2.5. Thermal Analysis. Differential scanning calorimetry curves were obtained with a Shimadzu TA-60WS (Shiumadzu Inc., Kyoto, Japan) thermal analysis system using 3−4 mg of the powder in open aluminum pans, in flowing air at 50 mL min^{-1}, and a heating rate of 10 °C min^{-1} from room temperature to 400 °C. An empty sealed aluminum pan was used as reference, and the calibration of the DSC instrument was carried out using indium as standard. Thermogravimetric analysis (TGA) was performed with a Shimadzu TGA-51 thermal analyzer using platinum pans, flowing air at 50 mL min^{-1}, and a heating rate of 10 °C min^{-1} from room temperature to 400 °C.

2.6. Transmission Electron Microscopy. The morphology of the inclusion complex was observed by transmission electron microscopy (TEM) using a Phillips CM 200 UltraTwin microscope, operating at 200 keV. The samples were dispersed in ultrapure water to form a suspension using a TestLab ultrasonicator for 2 h. Then, aliquots of the suspension were dropped on carbon-coated copper grids, and the extra solution was air-dried at room temperature. Staining of the samples with heavy metals solutions was unnecessary.

2.7. Solubility Studies. Phase solubility diagrams were built following a previously reported procedure.[20] The concentrations of 2OHBP were determined at 259 nm using an UV−vis Cary-50 Varian spectrophotometer with temperature controller. Baseline was established for each measurement by replacing an aqueous solution of βCD in the reference compartment at the same concentration of the sample. The experiments were carried out in triplicate.

The equilibrium solubility of 2OHBP (with and without FD), the PM, and FD 2OHBP:βCD samples were measured using the saturation *shake-flask* method at 37 °C. More details of these measurements are given as Supporting Information.

2.8. HPLC Measurements. Chromatographic experiments were performed using a Gilson 322 series pump (Gilson Inc., Middleton, WI) with a Rheodyne 7725i sample injector, a reverse phase Luna C18 (2) column (5 μm, 250 mm × 4.6 mm) from Phenomenex, a Gilson 152 UV−vis detector, and a Therma-Sphere TS-130 temperature controller. For the apparent formation constants determinations the mobile phase composition was MeOH−water (60:40, v/v), and different temperatures (25.0, 30.0, 35.0, 40.0, and 45.0 ± 0.1

°C) were employed. βCD was dissolved in the mobile phase, and 2OHBP was injected into the column, with an injection volume of 20 μL.

2.9. Molecular Modeling. The molecular geometries of βCD, 2OHBP, and the inclusion complexes were fully optimized using the PM6 model (Parametric Model 6).[21] Initial coordinates of βCD were obtained from crystallographic data.[22] The vibrational frequencies were calculated to ensure that the stationary points were true minima. A previously adopted procedure was followed to simulate the inclusion process,[23] and two possible orientations were considered: the "head up" and "head down" orientations, in which 2OHBP initially points toward the primary and the secondary hydroxyls of βCD, respectively. The PM6 optimized geometries of minimum energy were further optimized at the Hartree−Fock level of theory (HF/6-31G(d,p)). Finally, single point energy calculations were performed using the B3LYP/6-31++G(d,p) method[24,25] (tight threshold). A natural bond orbital (NBO)[26] analysis was carried out also at the B3LYP/6-31++G(d,p) level in order to quantify relevant interactions in the inclusion complexes. All the calculations were performed with MOPAC 2009 and GAUSSIAN 03 software packages.[27]

3. RESULTS AND DISCUSSION

3.1. FT-IR Measurements. The FT-IR spectra of (a) 2OHBP, (b) βCD, and the samples prepared by (c) FD and (d) PM are shown in Figure 1. Because of the FTIR spectra are
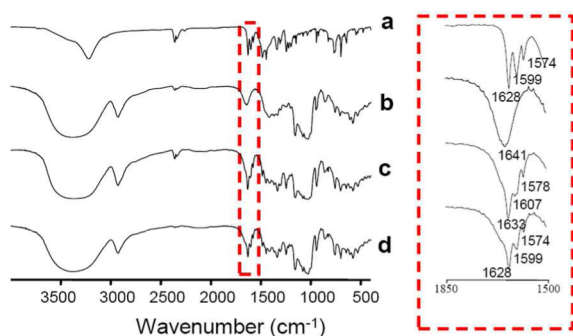
Figure 1. FT-IR spectra of (a) free 2OHBP, (b) βCD, (c) FD 2OHBP:βCD, and (d) PM 2OHBP:βCD.

very rich in bands, the vibrational analysis was performed taking into account the bands that showed the most significant shifts. The carbonyl stretching signal (νC=O) of free 2OHBP is located at 1628 cm^{-1}, while the peaks observed at 1599 and 1574 cm^{-1} can also be assigned to νC=O, coupled with in-plane C−H deformations and C−C stretching from aromatic ring modes (Figure 1a).[28] The FTIR spectrum of the FD 2OHBP:βCD sample (Figure 1c) shows a small shift of these signals to higher frequencies (1633, 1607, and 1578 cm^{-1}). This can be attributed to a slight reinforcement of the C=O bond of the drug in the complex since the intramolecular H-bond presents in the free drug crystal lattice[29] is weakened upon complexation. This observation suggests that the carbonyl group of 2OHBP is involved in the inclusion process. Conversely, no significant changes are observed in the PM spectrum (Figure 1d) which is the overlay of the of pure βCD and 2OHBP spectra. Then, from the spectroscopic analysis a possible interaction between the guest drug and βCD in solid state can be observed.

3.2. Powder X-ray Diffraction. The powder XRD patterns of (a) 2OHBP, (b) βCD, and the binary systems prepared by (c) FD and (d) PM are presented in Figure 2. The
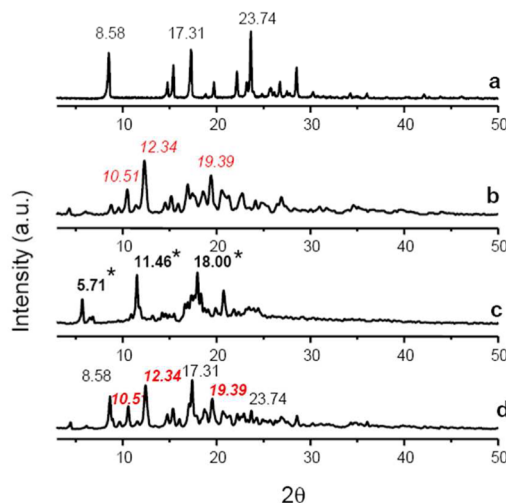

Figure 2. Powder X-ray diffractograms of (a) free 2OHBP, (b) βCD, (c) FD 2OHBP:βCD, and (d) PM samples. The main diffractions are labeled in black (2OHBP), red (βCD), and bold black with asterisks (FD 2OHBP:βCD).

diffractogram of 2OHBP is coincident with the previously reported one.[29] In addition, the diffractograms of the pure 2OHBP and the FD free drug are identical (Figure S1), indicating that this process does not affect the crystallinity of 2OHBP. The diffraction pattern of βCD also shows the crystalline nature of this compound. In the case of the PM sample, its XRD pattern is a direct superposition of fractions of the individual pattern of the free host and guest. However, a lower intensity and a broadening of the diffraction peaks of 2OHBP are observed while the characteristic peaks of βCD remain practically unchanged. This fact could be indicative of an alteration of the drug crystallinity after mixture in PM sample. Moreover, the diffractogram of the FD 2OHBP:βCD sample presents a different pattern from that of pure 2OHBP and βCD. The new peaks (diffractions labeled with asterisks) observed in Figure 2c are revealing that a new phase is obtained. This observation can be taken as an evidence for the presence of a true inclusion complex in the FD 2OHBP:βCD.[30] Caira has proposed a methodology for the characterization of CDs inclusion complexes based on the observation that within an isostructural series of inclusion complexes the general features of the powder XRD patterns are the same, regardless of the nature of the included drug.[31] The observed diffractions for the complex near 5.7, 11.5, and especially the intense peak at 18 are in agreement with the pattern of the dimeric head-to-head βCD complexes with a channel-type packing structure. For this reason, this type of structure can be proposed for the 2OHBP:βCD inclusion complex in solid state.

3.3. Thermal Analysis. The thermal characterization of 2OHBP, βCD, PM, and FD binary mixtures was performed. The DSC and TGA curves of the samples are illustrated in Figure 3. 2OHBP shows a sharp endothermic peak at 40.68 °C, corresponding to the melting process, while the TGA curve (Figure 3a) exhibits a major weight loss (97.33%) between 78.15 and 235.58 °C, corresponding to the decomposition of the drug. Two peaks associated with this weight loss are found
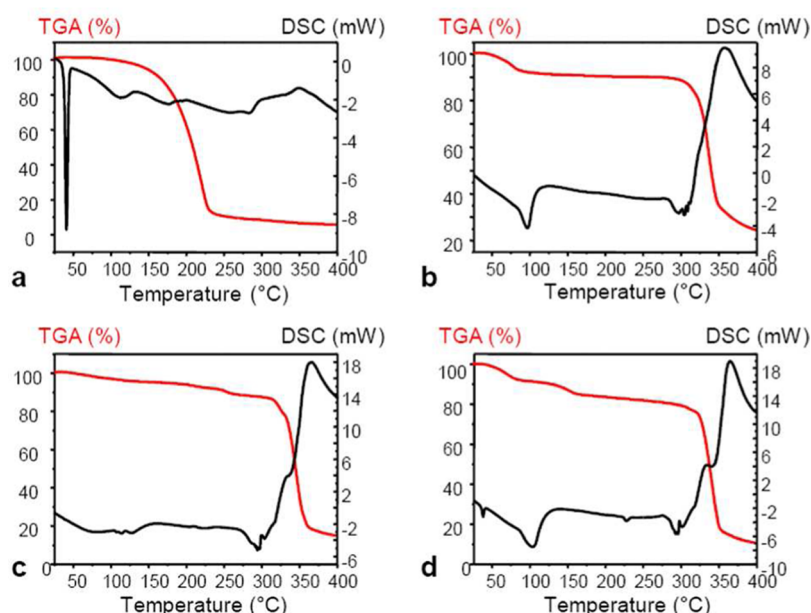
Figure 3. DSC (black lines) and TGA (red lines) curves of (a) free 2OHBP, (b) βCD, (c) FD 2OHBP:βCD, and (d) PM 2OHBP:βCD.

at 112.79 and 176.90 °C. The DSC analysis of βCD shows an endothermal event at 96.80 °C associated with a mass loss of 11.27% (calcd 11.25%) in the TGA curve (Figure 3b). This value is related to the loss of eight water molecules from the βCD cavity.[32] Additionally, an endothermic band is also observed at 297.35 °C associated with a mass loss (88.49%) due to the decomposition of this compound. In the FD 2OHBP:βCD sample (Figure 3c) the melting peak of 2OHBP disappears, and the event corresponding to the dehydration of βCD shifts to higher temperatures (113.98 °C). The latter event is associated with a weight loss of 5.29% (calcd 5.12%), related to the loss of four water molecules. The dehydration process was confirmed by the VT-FTIR spectra (Figure S2) which exhibit a decreasing intensity in the bands derived from water molecules (3367, 1636, and 935 cm^{-1}). Then, a second weight loss is observed in the TGA curve corresponding to the benzophenone decomposition. This event is observed in the DSC curve as an endothermal signal at 222.85 °C. These results suggest that the inclusion complex increase the thermal stability of 2OHBP. On the contrary, no significant changes are observed in the temperature of the βCD degradation in the FD sample (294.42 °C). The DSC curve of the PM sample (Figure 3d) presents the endothermal events corresponding to the melting process of 2OHBP, the dehydration of βCD, and the decomposition of 2OHBP and βCD. It must be noticed that the melting endotherm of the drug is broader in the PM than the corresponding in the 2OHBP sample. This fact is in agreement with the powder XRD, where a decrease in the crystallinity degree of the drug is observed.

3.4. TEM Analysis. Transmission electron microscopy observations are frequently employed to investigate the formation of micro and nanoaggregates of CDs and its inclusion complexes.[19,33] The aggregation behavior of these compounds may affect several properties such as the transport and delivery of the drugs; thus, the analysis of these aggregates should be considered in the study of CD inclusion complexes. In Figure 4a, the TEM image of the FD 2OHBP:βCD inclusion complex in water ($\sim$3 mM) is shown. This figure shows irregular nanoparticles with a discoidal shape and an average
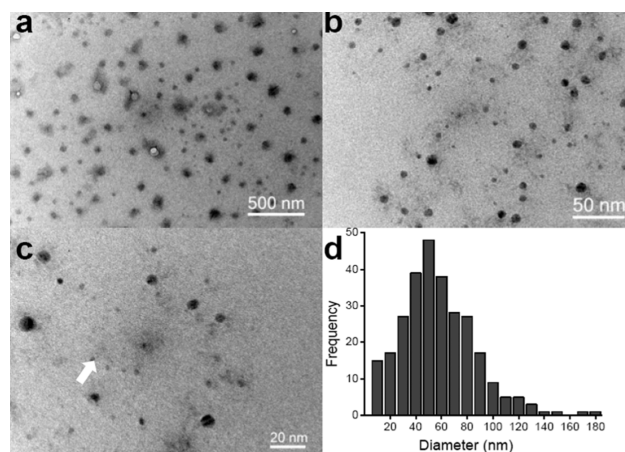
Figure 4. TEM images of (a−c) FD 2OHBP:βCD sample in water ($\sim$3 × 10^{-3} M). (d) Histogram showing the size distribution of the inclusion complex particles.

diameter of 57 nm. A similar type of aggregate has been previously observed for other CD inclusion complexes.[34−36] It can also be observed from this figure that smaller nanoparticles with diameters of about 2 nm are present (Figure 4c). Considering that the diameter of anhydrous native βCD is 1.54 nm,[30] the presence of monomers or even dimers of the inclusion complex can be proposed in the analyzed sample. In addition, it is known that the size of the CD-containing aggregates strongly depends on temperature and ultrasound intensity during sample preparation.[37] The aggregates were observed at room temperature and without sonication, but the highest populations were obtained after 2 h of sonication at 40 °C. No aggregates were observed by TEM in aqueous dispersion of the individual drug and βCD with the same sample preparation, suggesting that the complexation with 2OHBP is responsible for the formation of these nanostructures.

3.5. Equilibrium Solubility. The equilibrium solubility of 2OHBP was measured in buffers and pure water in order to

quantify the effect of the interaction with βCD. The solubility of 2OHBP in pure water is very low (50 $\pm$ 5 μM) and according to the USP can be considered as a practically insoluble drug.[38] The FD process increase this value up to 107 $\pm$ 7 μM. Moreover, an even higher aqueous solubility value is obtained for the FD 2OHBP:βCD inclusion complex (148 $\pm$ 12 μM), indicating that the interaction of the drug with βCD enhances it solubility more efficiently than the FD process. It is important to note that the measured solubility of the inclusion complex also includes the free drug. For the PM sample, only a small increase in the solubility is observed, 78 $\pm$ 3 μM, possibly due to the loss of crystallinity during sample preparation, as was observed by PXRD.

The solubility of the analyzed samples was also measured in two buffers, at different pH values (1.5 and 7.4), and the results are reported in Table S1. It can be seen from this table that the same trend measured in pure water is observed in the buffers.

3.6. Phase Solubility Diagrams and Apparent Formation Constants. The apparent formation constants (K_C) of the 2OHBP:βCD inclusion complex in aqueous solutions were obtained from phase-solubility diagrams, relating the drug solubility with the βCD concentration. The concentration of 2OHBP was measured by UV−vis spectroscopy, and an increase in the absorption intensity was observed at increasing concentration of βCD (Figure S3). This is indicative that the drug solubility is enhanced through the formation of a complex with βCD. The system can be classified as B_S type (Figure S4), which means that there is a linear increase of the drug solubility up to a certain concentration level of βCD ($\sim$0.9 mM); then a plateau is reached, indicating that the complex has a limited solubility.[39] This kind of behavior has previously been observed for the 2ClBP:βCD inclusion complex, but with a higher βCD concentration limit (1.2 mM).[20] From the linear segment of a B_S-type diagram, the stoichiometric ratio and the formation constant can be determined using the equation

$$S_t = S_0 + \frac{K_C S_0 [\beta CD]}{1 + K_C S_0} \tag{1}$$

where S_t and S_0 are the total and intrinsic drug solubility (in absence of βCD), respectively. If the slope of the graphical representation of eq 1 is less than 1, the stoichiometry of the complex is 1:1, and the K_C values can be calculated from the slope and intercept.[39] The results obtained by treating the experimental data with the above equation are listed in Table 1. The formation constants were measured in the range of 25−45 °C, and in all the cases the slopes of the fitted equations were smaller than 1 (between 0.211 and 0.591), indicating a 1:1 stoichiometry of the complex in solution. Moreover, from

Table 1. Apparent Formation Constants of the 2OHBP:βCD Inclusion Complex Obtained from Phase-Solubility Diagrams (K_C) and Chromatographic Measurements (K_F) at Different Temperatures

T (°C)	K_C (M^{-1})	R^2 [a]	K_F (M^{-1})	R^2 [b]
25	851 $\pm$ 45	0.986	144 $\pm$ 22	0.992
30	2191 $\pm$ 48	0.997	163 $\pm$ 29	0.989
35	4509 $\pm$ 322	0.992	136 $\pm$ 16	0.995
40	5159 $\pm$ 250	0.993	68 $\pm$ 17	0.997
45	3136 $\pm$ 331	0.983	34 $\pm$ 7	0.987

[a]R^2 is the correlation coefficient from linear fit of eq 1. [b]R^2 is the correlation coefficient from linear fit of eq 3.

Table 1 it can be observed that the K_C values increase with the temperature up to 40 °C and then decreases. This kind of behavior suggests that the enthalpy ($\Delta H°$) and entropy ($\Delta S°$) changes of the inclusion process are temperature dependent, and then the $\Delta C_p° \neq 0$.[40] For this reason, the thermodynamic quantities of this process must be obtained from the nonlinear van't Hoff equation:

$$R \ln K = -\frac{\Delta H° + (T - 298.15)\Delta C_p°}{T} + \Delta C_p° \ln\left(\frac{T}{298.15}\right) + \Delta S° \tag{2}$$

In eq 2, when $\Delta C_p° = 0$ the classical expression of van't Hoff equation is obtained. The $\Delta H°$, $\Delta S°$, $\Delta C_p°$, and the Gibbs energy change ($\Delta G°$) at 298.15 K of the encapsulation of 2OHBP into the βCD cavity in aqueous solution were calculated using eq 2, and the following results were obtained:

$$\Delta H° = 95.86 \text{ kJ/mol}$$

$$\Delta S° = 377 \text{ J/(K mol)}$$

$$\Delta C_p° = -15.42 \text{ kJ/(K mol)}$$

$$\Delta G° = -16.69 \text{ kJ/mol}$$

The thermodynamic parameters are associated with different types of driving forces of the inclusion process. It is known that electrostatic and van der Waals interactions, hydrogen bonding, hydrophobic effects, and the release of high energy water molecules from the CD cavity, among others, are the main forces governing the inclusion of solutes into a CD.[40,41] The hydrophobic interactions are related to positive or near zero $\Delta H°$ and large positive $\Delta S°$, indicating the inclusion process is entropy driven, while the van der Waals forces are related to negative $\Delta H°$ and $\Delta S°$ values. The results obtained for the studied inclusion complex show that the encapsulation is entropically favored ($\Delta S° > 0$) but with an unfavorable enthalpic term ($\Delta H° > 0$) in aqueous solution. It can be concluded then that the studied inclusion process is endothermic and entropically driven, and it is governed essentially by hydrophobic effects. Although the complexation of organic solutes with CDs is usually an exothermic process, positive $\Delta H°$ values were obtained for the inclusion complexes of some flavonoids with CDs.[42,43] Some authors suggested that positive $\Delta H°$ values are due to strong interactions of the free solute with its solvent shell. When the inclusion complex is formed, this solvent shell is broken, leading to an unfavorable enthalpic change.[43] This desolvation process would be responsible for the high positive enthalpy change observed. Moreover, the $\Delta C_p°$ is negative as usually found in the inclusion of hydrophobic solutes into CDs.[40]

The apparent formation constant of the 2OHBP:βCD inclusion complex were also obtained through HPLC with a mobile phase of MeOH-water (60:40, v/v). Samples of 2OHBP were injected in the HPLC column in the presence of βCD in the mobile phase and the change in the solute's capacity factor (k') with the βCD concentration ($[\beta CD]_m$) was analyzed using the relationship[44]

$$\frac{1}{k'} = \frac{1}{k'_0} + K_F \frac{[\beta CD_m]}{k'_0} \tag{3}$$

k'_0 is the solute capacity factor without βCD in the mobile phase, and K_F is the complex formation constant measured from chromatographic data. All the $[\beta CD_m]$ employed to analyzed the chromatographic data were corrected taking into account the MeOH:βCD formation constant.[44] The plots of 1/k' versus ($[\beta CD_m]$) are shown in Figure S5, and the K_F values, calculated from the slope and intercept of the straight lines, are reported in Table 1. It can be seen that the K_F values are lower that the corresponding K_C. For example, at 25 °C K_F is equal to 144 M^{-1} while K_C is equal to 851 M^{-1}. This result is expected since the addition of MeOH reduced the solution polarity favors the solubility of 2OHBP, and the affinity of the drug for the CD cavity is reduced.

Since there is no linear relationship between ln K_F and $1/T$, the thermodynamic parameters of the inclusion process in MeOH−water at 298.15 K were also calculated using eq 2, and the following results were obtained:

$$\Delta H° = -3.815 \text{ kJ/mol}$$

$$\Delta S° = 28.63 \text{ J/(K mol)}$$

$$\Delta C_p° = -10.24 \text{ kJ/(K mol)}$$

$$\Delta G° = -12.35 \text{ kJ/mol}$$

These values indicate that the reaction is exothermic and that both $\Delta H°$ and $\Delta S°$ are favorable to the complex formation in MeOH−water solution. It is important to notice that the relative contribution to the $\Delta G°_{298 K}$ of the terms $\Delta H°$ and $T\Delta S°$ is 30% and 70%, respectively. From these values, a balance between hydrophobic effects ($\Delta H° \sim 0$; $\Delta S° > 0$) and van der Waals forces ($\Delta H° < 0$; $\Delta S° < 0$) can be proposed, with a small predominance of the former interactions. Moreover, in the MeOH−water mixture the observed $\Delta S°$ is significantly lower than the corresponding $\Delta S°$ value measured in aqueous solution. When MeOH is added to the reaction medium, the hydrophobic part of the drug will be surrounded, in part, by the methanol molecules. These molecules replace the ordered aqueous microenvironment, resulting in a decrease of the $\Delta S°$ obtained in a completely aqueous medium.[20,45]

3.7. Molecular Modeling Results. The structural characteristics of the 2OHBP:βCD inclusion complex were further investigated using quantum mechanics calculations. The stabilization energy (ΔE) of the inclusion process was calculated as follows:

$$\Delta E = E_{2OHBP:\beta CD} - (E_{2OHBP} + E_{\beta CD}) \qquad (4)$$

Two possible orientations were considered for the complex formation: the head down and the head up. The PM6 results indicate that the head up orientation is energetically favorable by 8 kJ/mol approximately. This energy difference calculated at the B3LYP/6-31++G(d, p)//HF/6-31G(d, p) level of theory is increased at 75 kJ/mol.

The 2OHBP:βCD molecular structure of minimum energy calculated at the HF/6-31G(d, p) level in the head up orientation is illustrated in Figure 5. The phenolic and carbonyl moieties of the BP molecule are completely embedded in the βCD cavity. The inclusion complexes are often stabilized by intermolecular weak interactions, such as hydrogen bonds. The NBO analysis identifies delocalization effects and the strength of these interactions can be quantified by means of the second-order stabilization energy (ΔE_{ij}). One intermolecular H-bond interaction was detected between the carbonyl (electron
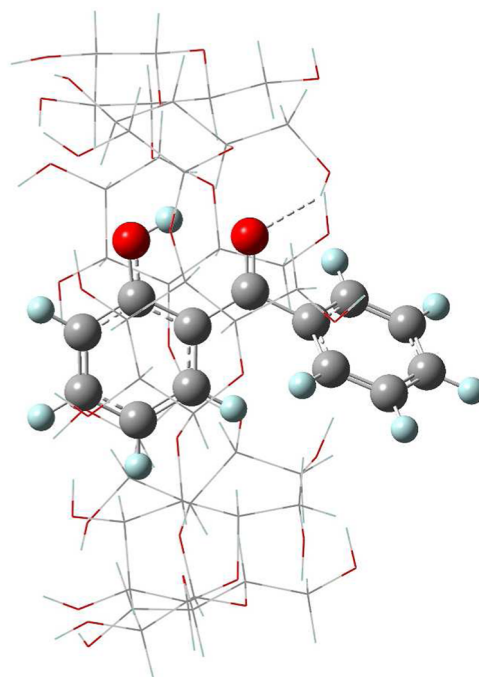
Figure 5. Molecular structure of the 2OHBP:βCD inclusion complex in the head up orientation calculated at the HF/6-31G(d,p) level of theory.

donor) of the 2OHBP and one OH group (electron acceptor) of βCD with a ΔE_{ij} = 5.43 kJ/mol, a bond length of 2.20 Å, and a bond angle of 147°. Moreover, the calculated stabilization energy for the intramolecular H-bond of 2OHBP was ΔE_{ij} = 46.94 kJ/mol, with a bond length of 1.82 Å and a bond angle of 140° in the isolated molecule, while in the complexed 2OHBP was ΔE_{ij} = 9.66 kJ/mol with a bond length of 1.85 Å and a bond angle of 140°. The decrease in the ΔE_{ij} value and the increase in the bond length indicate that the intramolecular H-bond of the drug is weakened upon inclusion on the βCD cavity, which is in good agreement with the observations made by FTIR spectroscopy.

4. CONCLUSIONS

The inclusion process of 2OHBP, a drug with a very low aqueous solubility, with βCD was investigated in solid state and in solutions of different nature. From the FTIR, PXRD, DSC, TGA, and TEM analysis it was observed that the inclusion complex can be obtained in solid state by the freeze-dried method. The complexation with βCD improved not only the aqueous solubility but also the thermal stability of the drug. In addition, it was found that the 2OHBP:βCD inclusion complex has the ability to form aggregates of irregular shape and nanometric size. The stoichiometry of this supramolecular system was 1:1 in solution. The formation constants of the complex in water (K_C) and in MeOH−water (K_F) were determined, and it was observed that $K_C > K_F$. In aqueous solution the encapsulation was endothermic and entropically driven while in MeOH−water was exothermic and driven both by enthalpy and entropy. From the molecular modeling analysis, the formation of an intermolecular H-bond between the C=O of the drug and one OH group of βCD was identified. Finally, the freeze-dried 2OHBP:βCD inclusion complex can be considered as a potential candidate for the design of a novel formulation of 2OHBP.

■ ASSOCIATED CONTENT

S **Supporting Information**

Experimental details and results of equilibrium solubility measurements; PXRD diffractograms of 2OHBP with and without freeze-dried; FT-IR spectra of the 2OHBP:βCD complex registered at different temperatures; UV−vis absorption spectra of 2OHBP with different concentrations of βCD; the phase solubility diagram of 2OHBP in the presence of βCD at 25 °C and the isotherms of $1/k$ versus effective βCD concentration. The Supporting Information is available free of charge on the ACS Publications website at DOI: 10.1021/acs.jpcb.5b01742.

■ AUTHOR INFORMATION

Corresponding Author

*Tel +54-266-4424689; Fax +54-266-4430224; e-mail misancho@unsl.edu.ar (M.I.S.).

Notes

The authors declare no competing financial interest.

■ ACKNOWLEDGMENTS

■ REFERENCES

(1) Demirkiran, O. Three New Benzophenone Glycosides with MAO-A Inhibitory Activity from Hypericum Thasium Griseb. *Phytochem. Lett.* **2012**, *5*, 700−704.

(2) Jo, Y. H.; Kim, S. B.; Ahn, J. H.; Liu, Q.; Hwang, B. Y.; Lee, M. K. Inhibitory Activity of Benzophenones from Anemarrhena Asphodeloides on Pancreatic Lipase. *Nat. Prod. Commun.* **2013**, *8*, 481−483.

(3) Trinh, B. T. D.; Nguyen, N. -T. T.; Ngo, N. T. N.; Tran, P. T.; Nguyen, L. -T. T.; Nguyen, L. -H. D. Polyisoprenylated Benzophenone and Xanthone Constituents of the Bark of Garcinia Cochinchinensis. *Phytochem. Lett.* **2013**, *6*, 224−227.

(4) MacIel-Rezende, C. M.; De Almeida, L.; Costa, É. D.; Pires, F. R.; Alves, K. F.; Junior, C. V.; Dias, D. F.; Doriguetto, A. C.; Marques, M. J.; Dos Santos, M. H. Synthesis and Biological Evaluation Against Leishmania Amazonensis of a Series of Alkyl-Substituted Benzophenones. *Bioorg. Med. Chem.* **2013**, *21*, 3114−3119.

(5) Kuete, V.; Tchakam, P. D.; Wiench, B.; Ngameni, B.; Wabo, H. K.; Tala, M. F.; Moungang, M. L.; Ngadjui, B. T.; Murayama, T.; Efferth, T. Cytotoxicity and Modes of Action of Four Naturally Occuring Benzophenones: 2,2′,5,6′-Tetrahydroxybenzophenone, Guttiferone E, Isogarcinol and Isoxanthochymol. *Phytomedicine* **2013**, *20*, 528−536.

(6) Perperopoulou, F. D.; Tsoungas, P. G.; Thireou, T. N.; Rinotas, V. E.; Douni, E. K.; Eliopoulos, E. E.; Labrou, N. E.; Clonis, Y. A. 2,2′-Dihydroxybenzophenones and Their Carbonyl N-Analogues as Inhibitor Scaffolds for MDR-Involved Human Glutathione Transferase Isoenzyme A1−1. *Bioorg. Med. Chem.* **2014**, *22*, 3957−3970.

(7) Borges, F.; Fernandes, E.; Roleira, F. Progress Towards the Discovery of Xanthine Oxidase Inhibitors. *Curr. Med. Chem.* **2002**, *9*, 195−217.

(8) Dewhirst, F. E. Structure-activity Relationships for Inhibition of Prostaglandin Cyclooxygenase by Phenolic Compounds. *Prostaglandins* **1980**, *20*, 209−222.

(9) Khanum, S. A.; Venu, T. D.; Shashikanth, S.; Firdouse, A. Synthesis of Some Newer Analogues of Substituted Dibenzoyl Phenol as Potent Anti-inflammatory Agents. *Bioorg. Med. Chem. Lett.* **2004**, *14*, 5351−5355.

(10) Doriguetto, A. C.; Martins, F. T.; Ellena, J.; Salloum, R.; dos Santos, M. H.; Moreira, M. E. C.; Schneedorf, J. M.; Nagem, T. J. 2,2′,4-Trihydroxybenzophenone: Crystal Structure, and Anti-inflammatory and Antioxidant Activities. *Chem. Biodiversity* **2007**, *4*, 488−499.

(11) Couteau, C.; Chauvet, C.; Paparis, E.; Coiffard, L. UV Filters, Ingredients with a Recognized Anti-inflammatory Effect. *PLoS One* **2012**, *7*, e46187.

(12) Parejo, P. G.; Zayat, M.; Levy, D. Highly Efficient UV-Absorbing Thin-Film Coatings for Protection of Organic Materials Against Photodegradation. *J. Mater. Chem.* **2006**, *16*, 2165−2169.

(13) Kawamura, Y.; Mutsuga, M.; Kato, T.; Iida, M.; Tanamoto, K. Estrogenic and Anti-androgenic Activities of Benzophenones in Human Estrogen and Androgen Receptor Mediated Mammalian Reporter Gene Assays. *J. Health Sci.* **2005**, *51*, 48−54.

(14) Cannavà, C.; Crupi, V.; Guardo, M.; Majolino, D.; Stancanelli, R.; Tommasini, S.; Ventura, C. A.; Venuti, V. Phase Solubility and FTIR-ATR Studies of Idebenone/sulfobutyl Ether β-Cyclodextrin Inclusion Complex. *J. Inclusion Phenom. Macrocyclic Chem.* **2013**, *75*, 255−262.

(15) Ferrazza, R.; Rossi, B.; Guella, G. DOSY-NMR and Raman Investigations on the Self-aggregation and Cyclodextrin Complexation of Vanillin. *J. Phys. Chem. B* **2014**, *118*, 7147−7155.

(16) Teixeira, M. G.; De Assis, J. V.; Soares, C. G. P.; Venaîncio, M. F.; Lopes, J. F.; Nascimento, C. S.; Anconi, C. P. A.; Carvalho, G. S. L.; Lourenço, C. S.; De Almeida, M. V.; et al. Theoretical and Experimental Study of Inclusion Complexes Formed by Isoniazid and Modified β-cyclodextrins: ¹H NMR Structural Determination and Antibacterial Activity Evaluation. *J. Phys. Chem. B* **2014**, *118*, 81−93.

(17) Frömming, K. H.; Szejtly, J. *Cyclodextrins in Pharmacy*; Kluwer Academic Publishers: Dordrecht, the Netherlands, 1994.

(18) Oishi, K.; Toyao, K.; Kawano, Y. Suppression of Estrogenic Activity of 17β-Estradiol by β-Cyclodextrin. *Chemosphere* **2008**, *73*, 1788−1792.

(19) Messner, M.; Kurkov, S. V.; Jansook, P.; Loftsson, T. Self-Assembled Cyclodextrin Aggregates and Nanoparticles. *Int. J. Pharm.* **2010**, *387*, 199−208.

(20) Sancho, M. I.; Gasull, E.; Blanco, S. E.; Castro, E. A. Inclusion Complex of 2-Chlorobenzophenone with Cyclomaltoheptaose (β-Cyclodextrin): Temperature, Solvent Effects and Molecular Modeling. *Carbohydr. Res.* **2011**, *346*, 1978−1984.

(21) Stewart, J. J. P. Optimization of Parameters for Semiempirical Methods V: Modification of NDDO Approximations and Application to 70 Elements. *J. Mol. Model.* **2007**, *13*, 1173−1213.

(22) Sharff, A. J.; Rodseth, L. E.; Quiocho, F. A. Refined 1.8-Å Structure Reveals the Mode of Binding of β-Cyclodextrin to the Maltodextrin Binding Protein a,b. *Biochemistry* **1993**, *32*, 10553−10559.

(23) Filippa, M.; Sancho, M. I.; Gasull, E. Encapsulation of Methyl and Ethyl Salicylates by β-Cyclodextrin. HPLC, UV-vis and Molecular Modeling Studies. *J. Pharm. Biomed. Anal.* **2008**, *48*, 969−973.

(24) Becke, A. D. Density-Functional Exchange-Energy Approximation with Correct Asymptotic Behavior. *Phys. Rev. A* **1988**, *38*, 3098−3100.

(25) Lee, C.; Yang, W.; Parr, R. G. Development of the Colle-Salvetti Correlation-Energy Formula into a Functional of the Electron Density. *Phys. Rev. B* **1988**, *37*, 785−789.

(26) Reed, A. E.; Curtiss, L. A.; Weinhold, F. Intermolecular Interactions from a Natural Bond Orbital, Donor-Acceptor Viewpoint. *Chem. Rev.* **1988**, *88*, 899−926.

(27) Frisch, M. J.; Trucks, G. W.; Schlegel, H. B.; Scuseria, G. E.; Robb, M. A.; Cheeseman, J. R.; Montgomery, J. A., Jr.; Vreven, T.; Kudin, K. N.; Burant, J. C.; et al. *Gaussian 03, Revision B.01*; Gaussian, Inc.: Pittsburgh, PA, 2003.

(28) Viana, R. B.; Santos, E. D. A.; Valencia, L. J.; Cavalcante, R. M.; Costa, E. B.; Moreno-Fuquen, R.; Da Silva, A. B. F. 4-Hydroxy-2,5-dimethylphenyl-benzophenone: Conformational Stability, FT-IR and Raman Investigation. *Spectrochim. Acta, Part A* **2013**, *102*, 386−392.

(29) Saraswat, K.; Prasad, R. N.; Ratnani, R.; Drake, J. E.; Hursthouse, M. B.; Light, M. E. Synthesis, Spectroscopic Characterization and Structural Studies of Mixed Ligand Complexes of Sr(II) and Ba(II) with 2-hydroxybenzophenone and Salicylaldehyde, Hydroxyaromatic Ketones or β-Diketones: Crystal Structure of 2-HOC$_6$H$_4$C(O)C$_6$H$_5$. *Inorg. Chim. Acta* **2006**, *359*, 1291−1295.

(30) Saenger, W. Cyclodextrin Inclusion Compounds in Research and Industry. *Angew. Chem., Int. Ed.* **1980**, *19*, 344−362.

(31) Caira, M. R. On the Isostructurality of Cyclodextrin Inclusion Complexes and Its Practical Utitlity. *Rev. Roum. Chim.* **2001**, *46*, 371−386.

(32) Kohata, S.; Jyodoi, K.; Ohyoshi, A. Thermal Decomposition of Cyclodextrins (α-, β-, γ-, and Modified β-CyD) and of Metal-(β-CyD) Complexes in the Solid Phase. *Thermochim. Acta* **1993**, *217* (C), 187−198.

(33) He, Y.; Fu, P.; Shen, X.; Gao, H. Cyclodextrin-based Aggregates and Characterization by Microscopy. *Micron* **2008**, *39*, 495−516.

(34) Messner, M.; Kurkov, S. V.; Brewster, M. E.; Jansook, P.; Loftsson, T. Self-assembly of Cyclodextrin Complexes: Aggregation of Hydrocortisone/Cyclodextrin Complexes. *Int. J. Pharm.* **2011**, *407*, 174−183.

(35) Shende, P. K.; Trotta, F.; Gaud, R. S.; Deshmukh, K.; Cavalli, R.; Biasizzo, M. Influence of Different Techniques on Formulation and Comparative Characterization of Inclusion Complexes of ASA with β-Cyclodextrin and Inclusion Complexes of ASA with PMDA Cross-linked β-Cyclodextrin Nanosponges. *J. Inclusion Phenom. Macrocyclic Chem.* **2012**, *74*, 447−454.

(36) Rajendiran, N.; Siva, S. Inclusion Complex of Sulfadimethoxine with Cyclodextrins: Preparation and Characterization. *Carbohydr. Polym.* **2014**, *101*, 828−836.

(37) Mazzaglia, A.; Ravoo, B. J.; Darcy, R.; Gambadauro, P.; Mallamace, F. Aggregation in Water of Nonionic Amphiphilic Cyclodextrins with Short Hydrophobic Substituents. *Langmuir* **2002**, *18*, 1945−1948.

(38) U.S. Pharmacopeia and the National Formulary, USP30-NF25, United States Pharmacopeia, 2008.

(39) Connors, K. A. Measurement of Cyclodextrin Complex Stability Constants. In *Comprehensive Supramolecular Chemistry*; Szejtli, J., Osa, T., Eds.; Elsevier: Oxford, UK, 1996; Vol. 3.

(40) Junquera, E.; Martin-Pastor, M.; Aicart, E. Molecular Encapsulation of Flurbiprophen and/or Ibuprophen by Hydroxypropyl-β-Cyclodextrin in Aqueous Solution. Potentiometric and Molecular Modeling Studies. *J. Org. Chem.* **1998**, *63*, 4349−4358.

(41) Alvira, E. A Continuum Model for van der Waals Interaction Between β-cyclodextrin and Linear Molecules: Part 1. *Chem. Phys. Lett.* **2007**, *439*, 252−257.

(42) Jullian, C.; Orosteguis, T.; Pérez-Cruz, F.; Sánchez, P.; Mendizabal, F.; Olea-Azar, C. Complexation of Morin with Three Kinds of Cyclodextrin. A Thermodynamic and Reactivity Study. *Spectrochim. Acta, Part A* **2008**, *71*, 269−275.

(43) Liu, B.; Li, W.; Nguyen, T. A.; Zhao, J. Empirical, Thermodynamic and Quantum-Chemical Investigations of Inclusion Complexation Between Flavanones and (2-hydroxypropyl)-cyclodextrins. *Food Chem.* **2012**, *134*, 926−932.

(44) López-Nicolás, J. M.; Núñez-Delicado, E.; Pérez-López, A. J.; Barrachina, A. C.; Cuadra-Crespo, P. Determination of Stoichiometric Coefficients and Apparent Formation Constants for β-cyclodextrin Complexes of Trans-resveratrol Using Reversed-Phase Liquid Chromatography. *J. Chromatogr. A* **2006**, *1135*, 158−165.

(45) Junquera, E.; Ruiz, D.; Aicart, E. Role of Hydrophobic Effect on the Noncovalent Interactions Between Salicylic Acid and a Series of β-cyclodextrins. *J. Colloid Interface Sci.* **1999**, *216*, 154−160.